



## **Sol-Gel Fabricated Transition Metal Cr<sup>3+</sup>, Co<sup>2+</sup> Doped Lanthanum Ferric Oxide (LFO-LaFeO<sub>3</sub>) Thin Film Sensors for the Detection of Toxic, Flammable Gases: A Comparative Study**

**\*<sup>1</sup>PRASHANT BHIMRAO KOLI, <sup>2</sup>KAILAS HARIBHAU KAPADNIS, <sup>3</sup>UDAY GANGADHAR DESHPANDE, <sup>1</sup>BALAJI PANDURANG MORE and <sup>4</sup>UMESH JAGANNATH TUPE**

<sup>1</sup>Research Centre in Chemistry, Arts, Commerce and Science College, Nandgaon, Taluka-Nandgaon, District- Nashik, (MH), India-423106. Affiliated to SPPU, Pune (MH), India.

<sup>2</sup>Research Centre in Chemistry and PG Department of chemistry, Loknete Vyankatrao Hiray Arts, Science and Commerce, College, Panchavati, Nashik-422003 Affiliated to SPPU, Pune (MH), India.

<sup>3</sup>Research Centre in Chemistry and PG Department of Chemistry, Pratap College, Amalner, Affiliated to KBC-NMU, Jalgaon (MH), India.

<sup>4</sup>Research Centre in Electronics and PG Department of Electronics, Loknete Vyankatrao Hiray Arts, Science and Commerce, College, Panchavati, Nashik-422003 Affiliated to SPPU, Pune (MH), India.

### **Abstract**

In this investigation we are reporting the rapid preparation of Perovskite LaFeO<sub>3</sub> thin films prepared by sol-gel synthesis followed by spin coating method. The structural properties of the spin coated LaFeO<sub>3</sub> thin films measured by X-ray Diffractometer which confirms the formation of monophasic, orthorhombic, Perovskite LaFeO<sub>3</sub> material. The morphological features of the films were explored by the ease of scanning electron microscopy, where the crystalline LaFeO<sub>3</sub> nanoparticles were observed. Energy dispersive spectroscopy was utilized for the determination of elemental composition. The electrical properties were carried out to confirm the typical semiconducting behaviour of LaFeO<sub>3</sub> p-type semiconductor. The thin films were subjected for gas sensing study, the material was found to be very efficient gas sensors for LPG, petrol vapour, CO<sub>2</sub>, methanol, ethanol, acetone gases. The main object was to discuss comparative study, means, what changes in parameters may be observed due to doping elements. Here undoped LFO sensor showed



### **Article History**

Received: 02 April 2020  
Accepted: 21 April 2020

### **Keywords:**

Flammable Gases;  
Gas Sensing;  
Petrol Vapours;  
Sol-Gel;  
Lfo-Sensors.

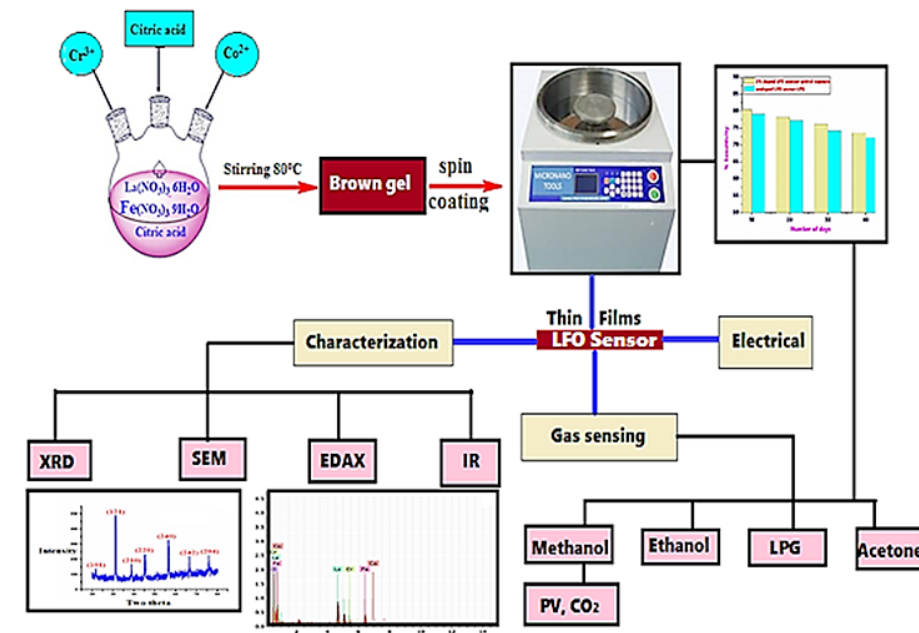
**CONTACT** Mr. Prashant Bhimrao Koli ✉ prashantkoli005@gmail.com 📍 Research Centre in Chemistry, Arts, Commerce and Science College, Nandgaon, Taluka-Nandgaon, District- Nashik, (MH), India-423106. Affiliated to SPPU, Pune (MH), India.



© 2020 The Author(s). Published by Oriental Scientific Publishing Company

This is an Open Access article licensed under a Creative Commons Attribution-NonCommercial-ShareAlike 4.0 International License  
Doi: <http://dx.doi.org/10.13005/msri/170110>

excellent sensitivity to methanol vapours, while doped LFO sensors found to very sensitive for petrol vapours. The enhanced sensitivity by doped LFO may attributed to increase surface area due to dopants. While all parameter essential for effective sensor were investigated in detail like, response recovery, reusability, selectivity of both the sensors.



Graphical presentation workflow for LFO sensors

**Introduction**

The material science now a days become the prime field of research due to excellent and promising application of the materials in the various field of science, engineering and technology. The use of material science, ceramics, nanomaterials in the diverse field is very huge because of their inherent properties such as high stability, accessibility, catalytic activity, thermal stability, cheap raw materials, easy synthesis route, high conversion factor, recycling ability, high surface area, tenable topography, agglomeration, high aspect ratio, agglomeration, mechanically stronger, etc.<sup>1-5</sup> Due to these natural marvellous properties the nanomaterials under the heading of material science are largely utilized in the various applications and processes such as energy storage, solar cells, photocatalysts, adsorbent, purification process, biosensors, effluent treatment, organic conversions, agriculture technology pharmaceuticals cosmetics,

medical agents, diagnosis, nanoenzymes, optical applications, bioimaging, catalytic convertors, in pollution control, bio combat process, green chemistry etc.<sup>6-10</sup>

In the current circumstance there is enormous increment in contamination because of fast urbanization and industrialization having a grievous effect on atmosphere and environment. Numerous specialists network attempting to take care of the contamination issue with the guide of material science and nanomaterials. Many research papers are posted by analysts with respect to the strategies to screen the toxic gases and fumes. The financially savvy sensors are accounted for, for example, thick, thin film sensors arranged by different simple, practical techniques. There are numerous techniques for manufacture of nanomaterial a portion of the mainstream strategy co-precipitation, sol-gel, combustion and so on. The nanomaterials arranged

by these technique can be used to get ready thick film/thin film sensors with the goal that combustible, lethal climatic and modern contaminations gases can be identified and checked. Dominant part of materials announced as thick/slender film sensors are bases on semiconducting transition metal oxide (STMO). In the current situation transition metal doped or F-block component doped sensors are additional normal in contrast with the undoped STMO. Despite the fact that the fantastic materials, for example, CNT bases sensors, nanocomposites, graphene oxide based, CNS doped, progress metal based STMO are accounted for by the analysts for the detecting of enormous number of gases.<sup>11-15</sup>

Next to this a portion of the intriguing reports have been accounted for by the analysts in gas detecting study. Mostly undoped and doped material and their correlation for the chose examine issue is novel pattern in the examination field. There are many explanation behind correlation investigation of undoped and doped material, for example, what is impact of dopant material as different properties is can be examined in contrast with the undoped material.<sup>16-18</sup>

The simple semiconducting oxide are modified in many ways and doping is one of the way to modify these material. Particularly 3d series elements are cheap and easy sources utilized for doping purpose. Many of the researchers explain their views regarding doping. Sasikala *et al.*, (2017) reported that the Ti doped LaFeO<sub>3</sub> is found to be excellent in electrical, magnetic properties were enhanced even though the band gap in Ti doped LFO is declined.<sup>19</sup> A. Paul Blessington co researchers (2015) reported that the effect Cr-substituted LaFeO<sub>3</sub> found be modified in Structural, Magnetic and Electrical conductivity properties.<sup>20</sup> R. Pushpa *et al.*, (2013) reported that calcium doped LaFeO<sub>3</sub> is very excellent in electronic properties.<sup>21</sup> L. Ma and co-researchers (2017) reported the enhanced sensing properties of acetic acid for cobalt doped LaFeO<sub>3</sub> sensor.<sup>22</sup>

In the present research we are reporting the comparative study of undoped and transition metal doped LaFeO<sub>3</sub> (LFO) thin film sensors prepared by sol- gel method. These sol-gel prepared sensors utilized for the gas sensing mechanism for the selected gases. The main purpose behind the doping

of the transition metal was to improve some catalytic properties of the prepared LFO sensors. In case of doped LFO sensors the surface area is found to be improved reported in Table 1. Due to this overall gas sensing results are found to be enhanced as reported in result and discussion section.

### Materials and Methods

All the reagents utilized in this research are analytical reagent grade purchased from Loba chemie, Mumbai. Chemicals utilized for the synthesis of undoped and doped LaFeO<sub>3</sub> are La (NO<sub>3</sub>)<sub>3</sub>, Fe (NO<sub>3</sub>)<sub>3</sub>, Cr (NO<sub>3</sub>)<sub>3</sub>, Co (NO<sub>3</sub>)<sub>3</sub>, (C<sub>6</sub>H<sub>8</sub>O<sub>7</sub>), double distilled water etc.

### Designing of Undoped LaFeO<sub>3</sub> Thin Film Sensor by Sol-Gel Method

Fabrication route of lanthanum ferric oxide sensors involves utilization of 0.01mol of La (NO<sub>3</sub>)<sub>3</sub> and 0.01 mol of Fe (NO<sub>3</sub>)<sub>3</sub> mixed thoroughly in 50 ml of distilled water. Into another beaker dissolve 0.0075 mol citric acid. Place lanthanum and ferric nitrate solution on magnetic stirrer and add to it citric acid solution drop by drop by adjusting the hating rate to 80°C. After 120 minutes brown colour sol was obtained. By continue heating to next 30 minutes the sol get converted to gel. This gel was then applied on earlier weighed glass film (1x2 cm), by spin coating method at 2000 rpm and nearly 110 seconds time required for complete coating of the film. The light brown coloured thin films then dried under IR lamp for 30 minutes and then keep in muffle furnace for 4 hours at 450°C. The undoped LaFeO<sub>3</sub> thin film was ready for further use.<sup>23</sup>

### Designing of Transition Metal Doped LaFeO<sub>3</sub> Thin Film Sensor by Sol-Gel Method

Fabrication route of doped lanthanum ferric oxide sensors involves utilization of 0.01mol of La (NO<sub>3</sub>)<sub>3</sub> and 0.01 mol of Fe (NO<sub>3</sub>)<sub>3</sub> mixed thoroughly in 50 ml of distilled water. Into another beaker dissolve 0.0075 mol citric acid. Now take 3% stoichiometric amount of Co (NO<sub>3</sub>)<sub>3</sub> and Cr (NO<sub>3</sub>)<sub>3</sub> and add these dopants to the lanthanum and ferric nitrate solution. Place lanthanum and ferric nitrate and dopant solution on magnetic stirrer and add to it citric acid solution drop by drop by adjusting the hating rate to 80°C. After 120 minutes grayish colour sol was obtained. By continue heating to next 30 minutes the

sol get converted to gel. This gel was then applied on earlier weighed glass film (1x2 cm), by spin coating method at 1800 rpm and nearly 120 seconds time required for complete coating of the film. The light brown coloured thin films then dried under IR lamp for 30 minutes and then keep in muffle furnace for 4 hours at 450°C. The Cr<sup>3+</sup>, Co<sup>2+</sup> doped LaFeO<sub>3</sub> thin film was ready for further use.

### Coating Measurement of the Films

The surface coating of the films was measured by using equation (1), thickness of the undoped LaFeO<sub>3</sub> films was perceived to be 3.41 μm, for doped LaFeO<sub>3</sub> the thickness of the film was found to be 3.51 μm measured by mass difference method. The thickness of the film was found in the thin region.

$$t = \Delta M / A \times \rho \quad \dots(1)$$

$\Delta M$  = Mass difference of the film before and after deposition.

$\rho$  = Composite density of undoped and doped lanthanum ferric oxide (LaFeO<sub>3</sub>)

A = Area of the film

## Results and Discussions

### X-ray Diffraction

The X-ray diffraction analysis of fabricated undoped and doped LaFeO<sub>3</sub> is as depicted in Figure 1 (a, b) respectively. The XRD analysis gives the 2θ peaks at 21.68, 31.29, 38.80, 45.2, 56.5, 66.50, 75.80 is assign to the reflection of the planes (101), (121), (210), (220), (240), (242), and (204) respectively for the two theta values. From this data the most intense peaks were analyzed for getting the mean particle size of the fabricated undoped and doped LFO sensors. The mean particle dimensions was formulated by Scherrer equation,  $D = K\lambda/\beta \cos \theta$ , in this equation, K=constant (0.9 to 1.39),  $\lambda$ =Radiation of wavelength (1.54 Å)  $\beta$ =FWHM (Full Width Half wave Maxima),  $\theta$ =Bragg angle of diffraction, D= mean particle Size. The mean particle size of undoped LaFeO<sub>3</sub> was found to be 32 nm and for doped LaFeO<sub>3</sub> the mean particle size was found to be 28 nm. The joint committee on powder diffraction standard (JCPDS) match scan data for lanthanum ferric oxide is (JCPDS No.37-1493), which confirms the formation of orthorhombic lanthanum ferric oxide (LaFeO<sub>3</sub>).<sup>24-25</sup>

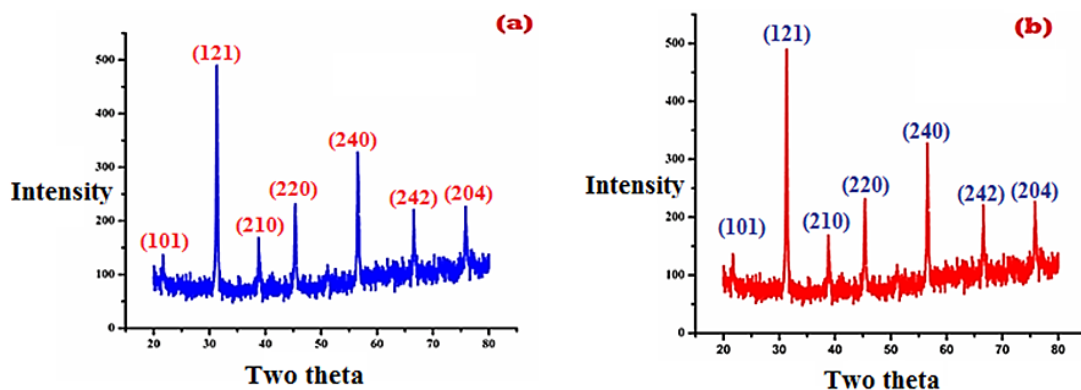


Fig.1:(a) XRD image of undoped LaFeO<sub>3</sub> (b) XRD image of Cr<sup>3+</sup>, Co<sup>2+</sup> doped LaFeO<sub>3</sub>

### Scanning Electron Microscopy

The scanning electron microscopy (SEM) is very useful technique to characterize the texture morphology of microscopic particles. The SEM images of undoped LaFeO<sub>3</sub> and Cr<sup>3+</sup>, Co<sup>2+</sup> doped LaFeO<sub>3</sub> (LFO) is as depicted in Figure 2 (a-d). In the SEM images of LFO material one can find that cubic crystals are very closely agglomerated and appeared as lumps of particles. Between these smaller lumps

the empty dark spots are appearing in the SEM images which are very small voids helpful for the adsorption phenomenon of gas sensing. Because of these cavities the smaller gases molecules may be occluded as adsorbates via physisorption or chemisorption.<sup>26-27</sup> The SEM images of both material appeared with the heterogeneous surface with varied sized nanoparticles agglomeration. The SEM images of both these material were utilized to find

out the surface area of prepared thin films by using Brunauer–Emmett–Teller (BET) equation for circular particles from equation 2.

Sw = Surface area, 6 (six) = constant, ρ (row) is the composite density of the materials, d= average particle size of functioning material.

$$Sw = 6 / \rho \times d \quad \dots(2)$$

**Table: 1 Surface area and mean nanoparticle size estimated with the aid of BET method for circular particles from SEM data**

Fabricated Sensor	Heating Temperature (°C)	Mean particle Size, D nm (XRD)	d nm (SEM)	Specific Surface Area in m <sup>2</sup> / g
Undoped LaFeO <sub>3</sub>	450	32	180	4.46 x 10 <sup>2</sup>
doped LaFeO <sub>3</sub>	450	28	205	6.70 X 10 <sup>2</sup>

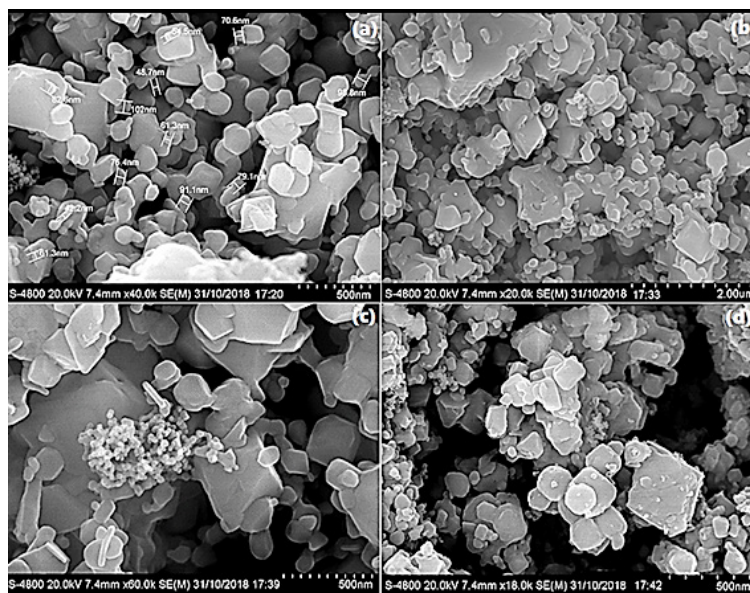


**Fig. 2 (a, b) SEM portrayal of undoped LaFeO<sub>3</sub> sensor, (c, d) SEM portrayal of Cr<sup>3+</sup>, Co<sup>2+</sup> doped LaFeO<sub>3</sub> sensor**

**Energy Dispersive Spectroscopy**

EDS is generally used to distinguish the essential arrangement of metals make component organization maps over an a lot more extensive territory together, these abilities give basic compositional data to a spacious assortment of materials. The scale is as appeared in Figure 3(a, b) from which one can discover incorporated material fixation which contains appropriate amount of present elements fabricated in LFO sensor. The doped

LFO sensor which contains Fe, Cr, La, Co and oxygen are observed in desired concentration in the EDAX image of doped LFO sensor. In the EDAX pictures the resolution of lanthanum and iron can be seen at 4.5 and 6.5 eV individually.<sup>28-29</sup> Where if there should be an occurrence of doped LaFeO<sub>3</sub> the dopants chromium and cobalt observed at 5.8eV and 7.0eV separately. The essential information is as appeared in Table 2 and Table 3.

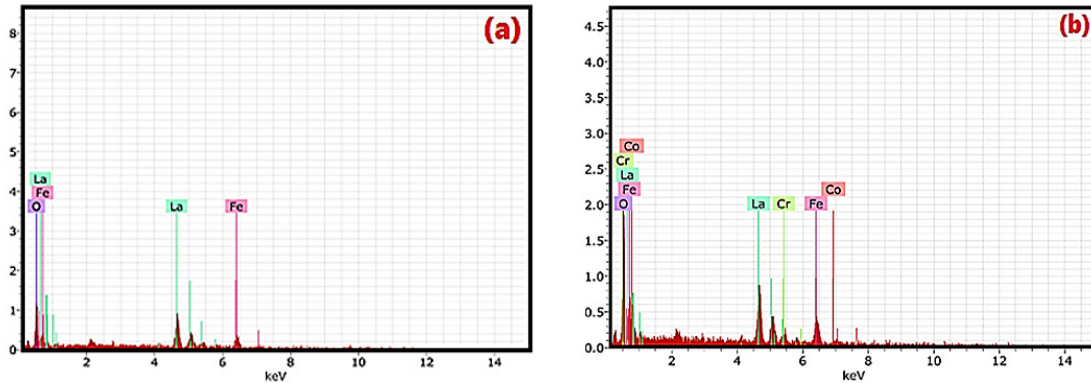


Fig.3: (a) EDS images of undoped LaFeO<sub>3</sub> (b) EDS images of Cr<sup>3+</sup>, Co<sup>2+</sup> doped LaFeO<sub>3</sub>

Table 2: Elemental composition of undoped LaFeO<sub>3</sub>

Element	Atomic Number	Series	Wt.%	At%
Oxygen	8	K	21.93	3.15
Iron	26	K	21.64	0.95
Lanthanum	57	L	56.43	1.12

Table 3: Elemental compositions of Cr<sup>3+</sup> Co<sup>2+</sup> doped LaFeO<sub>3</sub>

S.N	Atoms	Weight %	Atomic %
01	Oxygen	67.15	3.38
02	Iron	16.72	0.86
03	Lanthanum	13.82	1.04
04	Cobalt	1.44	0.22
05	Chromium	0.87	0.12

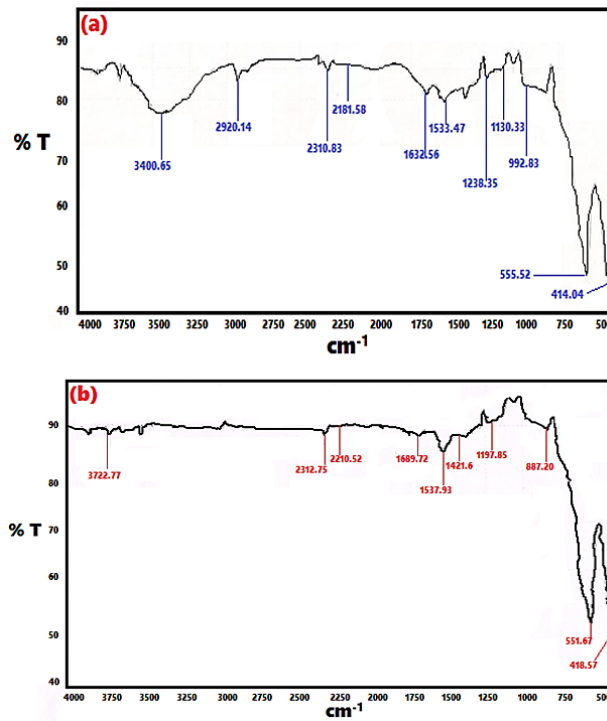


Fig.4: FT-IR spectrum of Cr<sup>3+</sup>Co<sup>2+</sup> doped lanthanum ferrite (LaFeO<sub>3</sub>)

### Fourier Transform Infra-Red Spectroscopy (FT-IR)

In nanomaterials the Fourier transform infra-red spectroscopy is can be utilized to investigate metal –oxygen stretching and bending vibrations. In case of metal oxide the metal and oxygen bounded in a particular geometry and their vibrations are unique that can be detected via FT-IR analysis. The FT-IR range of undoped  $\text{LaFeO}_3$  is as represented in Figure 4 (a, b). The trademark extending frequencies of La-O and Fe-O are as represented in the said figure. The FTIR range of incorporated material  $\text{LaFeO}_3$  doped by  $\text{Cr}^{3+}$  and  $\text{Co}^{2+}$  is depicted in Figure 4. The water of crystallization peak is appeared at  $3722.77 \text{ cm}^{-1}$ . According to literature the metal oxygen vibration bands are appeared nearly  $1000 \text{ cm}^{-1}$  due to strong affinity of bonding in metal oxide linkages. The fixed lanthanum- oxygen vibration in LFO sensor is observed at  $551.67 \text{ cm}^{-1}$ , while iron-oxygen vibration stretch is recorded at  $418.57 \text{ cm}^{-1}$ , While  $887.20 \text{ cm}^{-1}$  may be attributed to Co-O vibration. The characteristic vibrational bands of other elements are also appeared in the FT-IR spectrum of doped LFO sensor. while some vibrational bands found to be missing from undoped LFO, FT-IR spectrum due to absent of dopants.<sup>30</sup>

### Electrical Resistivity and Temperature Effect on Lanthanum-Ferrite Sensors (LFO-Sensors)

The gas detecting features of undoped and doped lanthanum ferrite examined at different raised temperature inside  $350^\circ\text{C}$  to  $30^\circ\text{C}$ . The electrical behaviour of the thick film sensor evaluated inside seeing air. The standard PTC nature of undoped and

doped lanthanum ferrite is as showed up in Figure 5 (a), (b). Here alongside dynamic decrease in heat the move in obstruction of the film was evaluated. Opposition increases firmly at early on arrange and deliberately with a movement of applied warmth hindrance reduces. The Figure 5 (a, b) shows lower in resistance with increase in heat on account of growing stream convey ability of the charge moving or as a result of lattice developments related with creating heat. Where the particles routinely approach, satisfactory for the trade the rate bearers and the conduction began with the guide of cross segment vibration.<sup>31-34</sup>

### Response and ppm Variation for Undoped and Doped LFO

The optimum % sensitivity undoped and doped  $\text{LaFeO}_3$  against the fixed parts per million concentration is as reflected in Figure 6 (a),(b). Here the percent sensitivity and gas concentration in ppm (0.5 g/L) for  $\text{CH}_3\text{-OH}$ ,  $\text{C}_2\text{H}_5\text{-OH}$ , LPG and petrol vapours is reported. As the gas concentration enhanced the optimum sensitivity is also found to be amplified due to more interaction of gas interaction on the surface of sensor. The voids, cavities or interstitial spaces present on the surface of sensor may be responsible to occlude or trap the more number of gas molecules via physisorption or chemisorption. Due to this effective interaction between adsorbate gases adsorbent sensor the amount of sensitivity is inflated. Thus every time with the insertion of more gas molecules on the surface of sensor, the response is expected to be intensified.

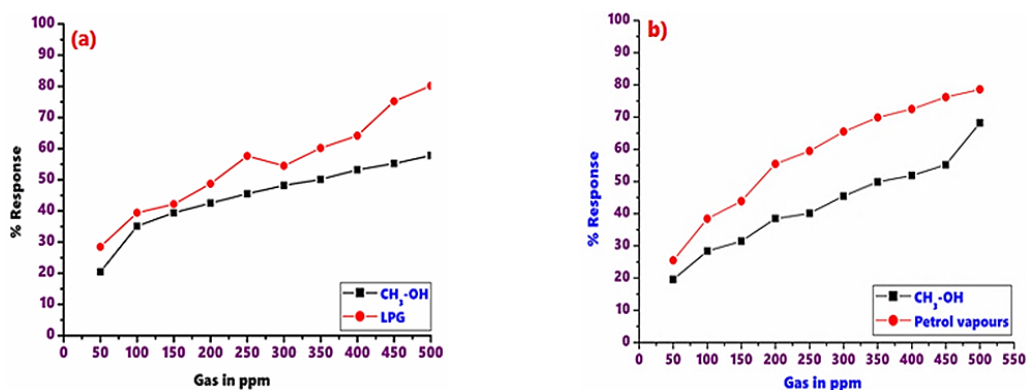


Fig.6: (a) optimum % sensitivity for  $\text{CH}_3\text{-OH}$  and LPG at 0.5 g/L gas concentration for undoped  $\text{LaFeO}_3$  (b) optimum % sensitivity for  $\text{CH}_3\text{-OH}$  and Petrol vapours at 0.5 g/L gas concentration for doped  $\text{LaFeO}_3$

**Sensitivity of Undoped and Doped Lanthanum Ferrites (LaFeO<sub>3</sub>)**

The affectability of different gases with temperature is as appeared underneath in Figure 7 and Figure 8 for undoped LaFeO<sub>3</sub> and doped LaFeO<sub>3</sub> thin film sensors respectively. The sensor undoped LaFeO<sub>3</sub> and Cr<sup>3+</sup>, Co<sup>2+</sup> doped LaFeO<sub>3</sub> were tested for gases, viz. CH<sub>3</sub>-OH, C<sub>2</sub>H<sub>5</sub>-OH, LPG, Acetone, CO<sub>2</sub> and petroleum fumes at the definite concentration

of 0.5g/L. By providing temperature to the sensor in nearness of specific gas the affectability and % response is evaluated. Contingent upon the sort of adsorption gas detecting adsorption may shift in sensors materials. From information of gas detecting study, the determined affectability for the gases of undoped and doped lanthanum ferrite thick film sensors is as appeared in Table 4.

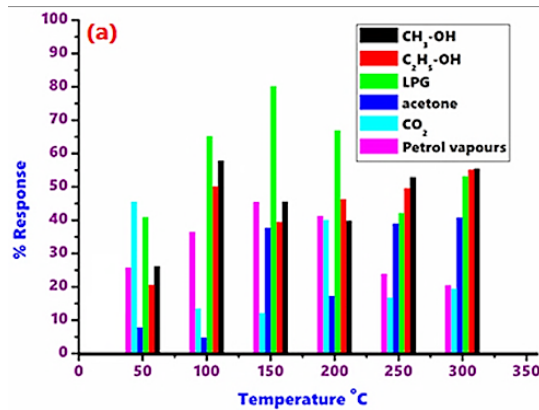


Fig.7: sensitivity at optimum temperature for undoped LaFeO<sub>3</sub>

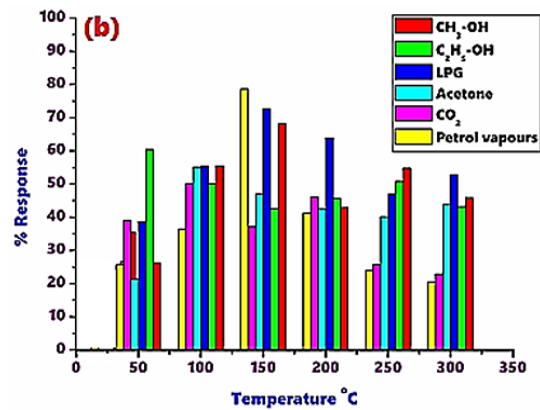


Fig.8: sensitivity at optimum temperature for doped LaFeO<sub>3</sub>

Table 4: report for gas response in undoped LaFeO<sub>3</sub> and 3% Cr<sub>3+</sub>, Co<sub>2+</sub> doped LaFeO<sub>3</sub> film sensor

Gas 0.5g/L	% S undoped LaFeO <sub>3</sub>	% S doped LaFeO <sub>3</sub>	Optimum sensing Temperature (°C) LaFeO <sub>3</sub>	Optimum sensing Temperature (°C) Doped LaFeO <sub>3</sub>
CH <sub>3</sub> -OH	57.80	68.20	100	150
C <sub>2</sub> H <sub>5</sub> -OH	55.12	60.45	300	50
LPG	80.15	72.78	150	150
Acetone	40.79	55.12	300	100
CO <sub>2</sub>	40.04	50.17	200	100
Petrol vapours	45.45	78.59	150	150

**Selectivity of Undoped and Doped LaFeO<sub>3</sub> Sensors**

The statistics obtained from the % selectivity calculations of the gases indicates that undoped LaFeO<sub>3</sub> appear to have optimum selectivity for LPG gas is 100 at 150°C, for CH<sub>3</sub>-OH gas the % selectivity observed at 72.11 for 100°C. For remaining gases viz. ethyl alcohol, acetone,

CO<sub>2</sub>, petrol vapours optimum selectivity was 68.17 (at 300°C), 50.89 (at 300°C), 49.98 (200°C), 56.70 (150°C) respectively. Among the reported data for LaFeO<sub>3</sub> sensor reflects that LPG, CH<sub>3</sub>-OH gases given outstanding response for the LFO. In addition to that the transition metal modified doped LaFeO<sub>3</sub> manifest enhance selectivity results in comparison to the undoped LaFeO<sub>3</sub>. The cause may be assign

to this results is improved surface area and declined band gap of modified LaFeO<sub>3</sub>. Here the doped LaFeO<sub>3</sub> (3% Cr<sup>3+</sup>, Co<sup>2+</sup>) exhibits the towering selectivity for petrol vapours i.e.100% at 150°C and LPG 92.81 % at 150°C. For remaining gases viz. methyl alcohol, ethyl alcohol, acetone, CO<sub>2</sub>,

selectivity was found to be 86.87 (at 150°C), 76.91 (at 50°C), 70.13( 100°C), 63.83 (100°C) respectively. The diagrammatic presentation of selectivity of undoped and doped lanthanum ferrite is as depicted in Figure 9.

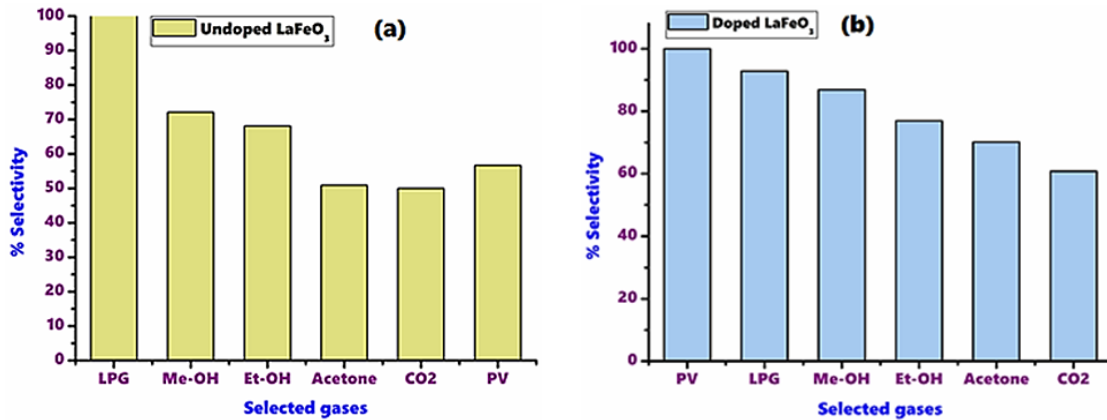


Fig.9: (a) optimum selectivity of various gases for undoped LaFeO<sub>3</sub> (b), optimum selectivity of various gases for doped LaFeO<sub>3</sub>

Table 5: synopsis for gas selectivity in undoped LaFeO<sub>3</sub> and 3% Cr<sup>3+</sup>, Co<sup>2+</sup>-doped LaFeO<sub>3</sub> thin film sensor

S.N	Selected Gas	Selectivity of undoped LaFeO <sub>3</sub>	Selectivity of doped LaFeO <sub>3</sub>
1	LPG	100	92.81
2	PV	56.70	100
3	CH <sub>3</sub> -OH	72.11	86.87
4	C <sub>2</sub> H <sub>5</sub> -OH	68.17	76.91
5	Acetone	50.89	70.13
6	CO <sub>2</sub>	49.98	63.83

**Response and Recovery for Undoped and Doped Lanthanum Ferrite Sensors**

Response and recovery parameter was performed for undoped and doped LaFeO<sub>3</sub> sensors. Figure 10 depicts the results acquire for both the sensors. For every sensor the optimum response of the gas, recovery of a gas from the sensor surface, stability of the sensors for wide range of thermal conditions and the reproducibility of the results are very prime investigations. As gas sensing phenomenon is associated with quick response to the gas and at

what time the particular gas is get recovered from sensor surface is very useful parameter to design the professional sensor. Hence all these parameters were investigated for those gases which given high response for the sensors under the investigation. Here the response, recovery and reproducibility tested for methyl alcohol, LPG in case of undoped LFO sensors. While these all parameters tested for methyl alcohol and petrol vapours for doped LFO sensors. Diagrammatic presentation of response and recovery is as depicted as below.

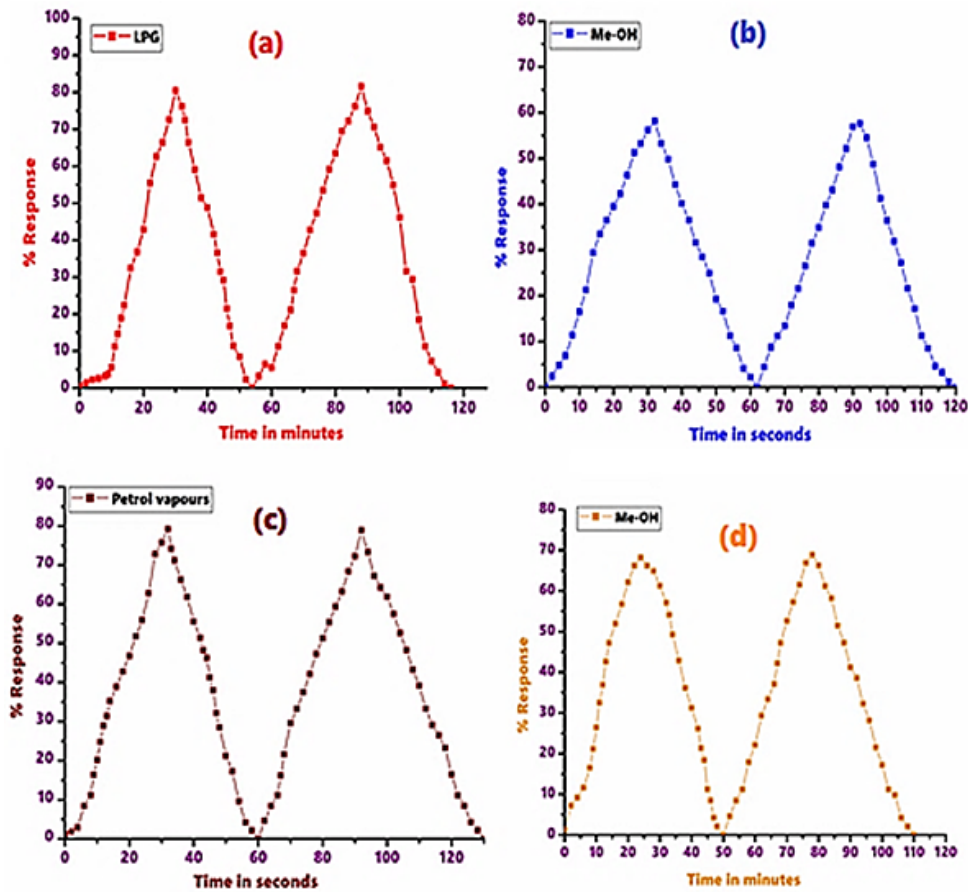


Fig.10: (a) Response and recovery curves for LPG, (b) for Me-OH gas in undoped LaFeO<sub>3</sub> (c) response and recovery graph for petrol vapours, (d) for Me-OH gas in doped LaFeO<sub>3</sub> sensor

Table 6: Synopsis of response and recovery for undoped and doped LaFeO<sub>3</sub> film sensors for selected gases

S.N	Gases	% S	Response Time (sec.)	Recovery Time (Sec.)
01	LPG	80.45	30	54
02	CH <sub>3</sub> -OH	58.20	32	62
03	Petrol Vapours	79.20	32	60
04	CH <sub>3</sub> -OH	68.22	24	50

(% S = sensitivity)

**Efficiency and Reusability of the Undoped and Doped Lanthanum Ferrite Sensors for High Responding Gases**

The undoped and doped lanthanum ferrite (LFO) sensors tested for high responding gases. As the efficiency of the sensor is prime investigation. Here

these both sensors undoped and 3% Cr<sup>3+</sup>, Co<sup>2+</sup> doped lanthanum ferrite sensors for LPG and petrol vapours. In this case, the sensors tested periodically at the interval of 10 days for these gases in four cycles. In undoped LFO sensor the high response given by LPG nearly 80% at 500 ppm concentration

in first cycle, then, the sensor utilized for LPG with 10 days interval and given the response 78.20%, similarly 76.15%, 73.56% response was recorded for third and fourth time respectively. In doped LFO the maximum response given by petrol vapours hence this gas optimised in the reusability test for doped LFO sensor. Here in the first run the response given by petrol vapours found to be 79.20%, similarly 77.14% in second usage after interval of 10 days and 74.20 %, 72.13% in third and fourth cycle for petrol vapours. For effective functioning of the sensor, it is very necessary the response must be reproducible.

Hence, both these sensors utilized for this function. Now here observation regarding declined in the response for every run after 10 days recorded, the reason could be assign to this observation is the decrease in the surface activeness of the sensors. As these sensors subjected frequently for the testing, the upper surface activity found to lower due to exposing of gas every time hence its adsorption property lowered. Therefore, steady decrease observed in the sensitivity response by these sensors. The reusability results depicted in Figure 11.

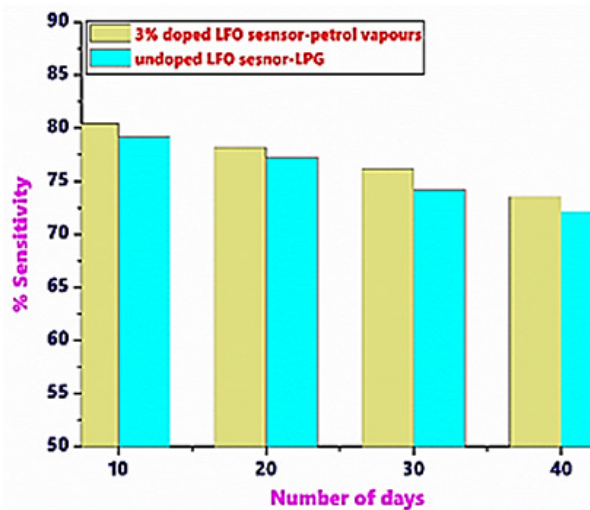


**Fig.11: Reusability of undoped and doped lanthanum ferrite (LFO) sensors for petrol vapours and LPG gases respectively**

#### Comparison of Results of Undoped and Doped Lanthanum Ferrite Sensors

As  $\text{LaFeO}_3$  consider as perovskite  $\text{ABO}_3$  oxide and researchers worked out on this material in various applications such as gas sensing, catalysis. According to the reports, this LFO material is excellent sensing material and it has ability to sense variety of gases. Majority of research papers showed that the LFO is good sensor for methanol, ethanol, acetone  $\text{H}_2\text{S}$  etc. But very rare reports are present on the LPG, petrol vapour gases. Hence, here we carry the work on these gases with the help of LFO undoped and transition metal doped LFO sensors for these gases. The material is effective sensors for these gases. Therefore, in the conclusion it can be confirm that LFO sensors are quite useful to sense the combustible gases like LPG and petrol vapours.

#### Conclusions

In the present research we have reported eco-friendly cost effective method for the fabrication of undoped transition metal doped LFO ( $\text{LaFeO}_3$ ) sensors, their comparative results are reported. The sensors utilized for the detection and monitoration of gases particularly LPG, petrol vapours. The sensors also utilized for some poisonous gases such as methyl alcohol, acetone and  $\text{CO}_2$ . However the sensors are found to be excellent for the flammable LPG, petrol vapours and almost 80% response is recorded for LFO sensors. In the overall concluding section it can be summarized as  $\text{Cr}^{3+}, \text{Co}^{2+}$  doped LFO sensor is very effective for the detection of petrol vapours in high thermal conditions.

### Acknowledgements

Authors are gratefully acknowledged to the SAIF UDCT, Jalgaon (M.S) for XRD, SEM and EDX. As well as SAIF Chandigarh (Punjab University) for FT-IR study. Authors are very thankful to Department of chemistry, ACS College, Nandgaon Department of Chemistry, L.V.H. College, Panchavati, Nashik and Department of electronics L.V.H. College, Panchavati, Nashik for providing necessary laboratory facilities.

### Funding

For this research work we do not received any fund or grand for the research work and this work is self-funded.

### Conflict of interest

Authors declared that they have no conflict of interest regarding this research article.

### References

1. Andrievski RA. Review of thermal stability of nanomaterials. *Journal of materials science*. 2014, 1; 49(4):1449-60.
2. Sharma N, Ojha H, Bharadwaj A, Pathak DP, Sharma RK. Preparation and catalytic applications of nanomaterials: a review. *RSC Advances*. 2015, 5 (66):53381-403.
3. Dhand C, Dwivedi N, Loh XJ, Ying AN, Verma NK, Beuerman RW, Lakshminarayanan R, Ramakrishna S. Methods and strategies for the synthesis of diverse nanoparticles and their applications: a comprehensive overview. *Rsc Advances*. 2015, 5(127):105003-37.
4. Ashraf MA, Peng W, Zare Y, Rhee KY. Effects of size and aggregation/agglomeration of nanoparticles on the interfacial/interphase properties and tensile strength of polymer nanocomposites. *Nanoscale research letters*. 2018, 1;13(1):214.
5. Koli PB, Kapadnis KH, Deshpande UG. Transition metal decorated Ferrosferric oxide ( $\text{Fe}_3\text{O}_4$ ): An expeditious catalyst for photodegradation of Carbol Fuchsin in environmental remediation. *Journal of Environmental Chemical Engineering*. 2019 Oct 1;7(5):103373.
6. Adole VA, Pawar TB, Koli PB, Jagdale BS. Exploration of catalytic performance of nano- $\text{La}_2\text{O}_3$  as an efficient catalyst for dihydropyrimidinone/thione synthesis and gas sensing. *Journal of Nanostructure in Chemistry*. 2019 Mar 1;9(1):61-76.
7. Shinde VS, Sawant CP, Kapadnis KH. Modified Sn-doped  $\text{LaCrO}_3$  nanostructures: focus on their characterization and applications as ethanol sensor at a lower temperature. *Journal of Nanostructure in Chemistry*. 2019 Sep 1;9(3):231-45.
8. Ngô C, Van de Voorde MH. Nanomaterials in Industrial Application. *In Nanotechnology in a Nutshell* 2014, 393-402.
9. Adole VA, Pawar TB, Jagdale BS. Aqua-mediated rapid and benign synthesis of 1, 2, 6, 7-tetrahydro-8H-indeno [5, 4-b] furan-8-one-appended novel 2-arylidene indanones of pharmacological interest at ambient temperature. *Journal of the Chinese Chemical Society*. 2020, 67(2):306-15.
10. Adole VA, More RA, Jagdale BS, Pawar TB, Chobe SS. Efficient Synthesis, Antibacterial, Antifungal, Antioxidant and Cytotoxicity Study of 2-(2-Hydrazineyl) thiazole Derivatives. *ChemistrySelect*. 2020 Mar 6;5(9):2778-86.
11. Raval NP, Shah PU, Shah NK. Adsorptive amputation of hazardous azo dye Congo red from wastewater: a critical review. *Environmental Science and Pollution Research*. 2016 1; 23(15):14810-53.
12. Gottschalk F, Sonderer T, Scholz RW, Nowack B. Modeled environmental concentrations of engineered nanomaterials ( $\text{TiO}_2$ , ZnO, Ag, CNT, fullerenes) for different regions. *Environmental science & technology*. 2009, 15;43(24):9216-22.
13. Zhao Z, Sun Y, Dong F. Graphitic carbon nitride based nanocomposites: a review. *Nanoscale*. 2015;7(1):15-37.
14. Ding F, Yang D, Tong Z, Nan Y, Wang Y, Zou X, Jiang Z. Graphitic carbon nitride-based nanocomposites as visible-light driven photocatalysts for environmental purification. *Environmental Science: Nano*. 2017; 4(7): 1455-69.
15. Sharma S, Hussain S, Singh S, Islam SS.

- MWCNT-conducting polymer composite based ammonia gas sensors: A new approach for complete recovery process. *Sensors and Actuators B: Chemical*. 2014 Apr 1; 194:213-9.
16. Wang Y, Zhang R, Li J, Li L, Lin S. First-principles study on transition metal-doped anatase TiO<sub>2</sub>. *Nanoscale research letters*. 2014 Dec 1;9(1):46.
  17. Chang SM, Liu WS. The roles of surface-doped metal ions (V, Mn, Fe, Cu, Ce, and W) in the interfacial behavior of TiO<sub>2</sub> photocatalysts. *Applied Catalysis B: Environmental*. 2014 Sep 1; 156:466-75.
  18. Hitkari G, Sandhya S, Gajanan P, Shrivash MK, Deepak K. Synthesis of chromium doped cobalt oxide (Cr: Co<sub>3</sub>O<sub>4</sub>) nanoparticles by co-precipitation method and enhanced photocatalytic properties in the visible region. *J. Mater. Sci. Eng*. 2018; 7(419).
  19. Sasikala C, Durairaj N, Baskaran I, Sathyaseelan B, Henini M, Manikandan E. Transition metal titanium (Ti) doped LaFeO<sub>3</sub> nanoparticles for enhanced optical structural and magnetic properties. *Journal of Alloys and Compounds*. 2017, 25; 712:870-7.
  20. Selvadurai AP, Pazhanivelu V, Jagadeeshwaran C, Murugaraj R, Muthuselvam IP, Chou FC. Influence of Cr substitution on structural, magnetic and electrical conductivity spectra of LaFeO<sub>3</sub>. *Journal of Alloys and Compounds*. 2015, 15; 646:924-31.
  21. Pushpa R, Daniel D, Butt DP. Electronic properties of Ca doped LaFeO<sub>3</sub>: A first-principles study. *Solid State Ionics*. 2013, 1;249:184-90.
  22. Ma L, Ma SY, Qiang Z, Xu XL, Chen Q, Yang HM, Chen H, Ge Q, Zeng QZ, Wang BQ. Preparation of Co-doped LaFeO<sub>3</sub> nanofibres with enhanced acetic acid sensing properties. *Materials Letters*. 2017 1;200:47-50.
  23. Yang Z, Huang Y, Dong B, Li HL. Controlled synthesis of highly ordered LaFeO<sub>3</sub> nanowires using a citrate-based sol-gel route. *Materials research bulletin*. 2006 2;41(2):274-81.
  24. Khetre SM, Jadhav HV, Jagadale PN, Kulal SR, Bamane SR. Studies on electrical and dielectric properties of LaFeO<sub>3</sub>. *Adv. Appl. Sci. Res*. 2011; 2(4):503-11.
  25. Khetre SM, Chopade AU, Khilare CJ, Kulal SR, Jadhav HV, Jagadale PN, Bangale SV, Bamane SR. Ethanol gas sensing properties of nano-porous LaFeO<sub>3</sub> thick films. *J Shivaji Univ (Sci Technol)*. 2014;41(2):250-5347.
  26. Lin Q, Lin J, Yang X, He Y, Wang L, Dong J. The effects of Mg<sup>2+</sup> and Ba<sup>2+</sup> dopants on the microstructure and magnetic properties of doubly-doped LaFeO<sub>3</sub> perovskite catalytic nanocrystals. *Ceramics International*. 2019 Feb 15;45(3):3333-40.
  27. Phokha S, Hunpratup S, Pinitsoontorn S, Putasaeng B, Rujirawat S, Maensiri S. Structure, magnetic, and dielectric properties of Ti-doped LaFeO<sub>3</sub> ceramics synthesized by polymer pyrolysis method. *Materials Research Bulletin*. 2015 Jul 1;67:118-25.
  28. Kumar RD, Thangappan R, Jayavel R. Synthesis and characterization of LaFeO<sub>3</sub>/TiO<sub>2</sub> nanocomposites for visible light photocatalytic activity. *Journal of Physics and Chemistry of Solids*. 2017 1; 101:25-33.
  29. Afifah N, Saleh R. Synthesis, characterization and catalytic properties of perovskite LaFeO<sub>3</sub> nanoparticles. *In Journal of Physics: Conference Series* 2016, Vol. 710, (1).
  30. Qi X, Zhou J, Yue Z, Gui Z, Li L. Auto-combustion synthesis of nanocrystalline LaFeO<sub>3</sub>. *Materials chemistry and physics*. 2003 Feb 3;78(1):25-9.
  31. Berchmans LJ, Sindhu R, Angappan S, Augustin CO. Effect of antimony substitution on structural and electrical properties of LaFeO<sub>3</sub>. *Journal of materials processing technology*. 2008 16; 207(1-3):301-6.
  32. Aono H, Ohmori J, Sadaoka Y. Effects of Sintering Atmosphere on Surface Structure and Electrical Properties of LaFeO<sub>3</sub> Prepared by Thermal Decomposition of La [Fe (CN)<sub>6</sub>]. 4H<sub>2</sub>O. *Journal of the Ceramic Society of Japan*. 2000 1; 108(1262):892-7.
  33. Korotcenkov G. Metal oxides for solid-state gas sensors: What determines our choice?. *Materials Science and Engineering: B*. 2007 Apr 25; 139(1):1-23.
  34. Zhao J, Liu Y, Li X, Lu G, You L, Liang X, Liu F, Zhang T, Du Y. Highly sensitive humidity sensor based on high surface area mesoporous LaFeO<sub>3</sub> prepared by a nanocasting route. *Sensors and Actuators B: Chemical*. 2013 May 1;181:802-9.